Published in the Russian Federation
Nanotechnology Research and Practice
Has been issued since 2014.
ISSN: 2312-7856
E-ISSN: 2413-7227
Vol. 10, Is. 2, pp. 74-94, 2016

DOI: 10.13187/nrp.2016.10.74
www.ejournal13.com

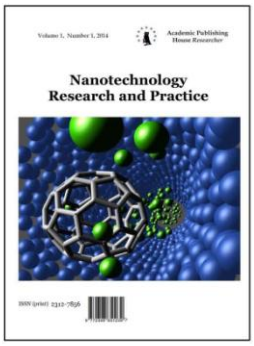

UDC 539.21:537; 658.567.1

Radiation effect on MHD mixed convection flow of a nanofluid through a porous medium in the presence of chemical reactions

Rajnish Kumar [a,*], Fauzia Raza [b], M. Subhas Abel [c]

[a] Department of Mathematics, Birla Institute of Technology, Mesra, Patna Campus, Bihar, India
[b] Department of Mathematics, Shri Venkateshwara University, Gajraula, U.P., India
[c] Department of Mathematics, Gulbarga University, Gulbarga, Karnataka., India

Abstract

An analysis is made to study radiation effect on MHD (magnetohydrodynamic) flow of CuO nanofluid in the presence of chemical reactions and mixed convection due to non-uniform heat source through a porous medium. The model for the nanofluid incorporates and analyses radiation parameter, Brownian motion, thermopheresis and magnetic field consequences. The nonlinear differential equations are solved for different values of governing parameters by using the function 'bvp4c' of MATLAB. A comparative study of our result with previously reported results is given. It is worth citing that the thermal boundary layer thickness reduces with rise in unsteadiness of parameter A. The decrease in value of thermal radiation Nr means an enhancement in Rosseland absorptivity.

Keywords: MHD, mixed convection, bvp4c, nanofluid, porous media, thermal radiation.

Introduction

A nanofluid is a liquid containing a dispersion of sub-micron solid particles through a distinctive length scale of order 1-100 nm. Nanofluids have attained an enormous interest owing to their place in the heat transfer processes of real life engineering applications, as discussed in the publication by Das et al [1] and Wang and Majumdar [2]. Nanofluid perception was first coined by Choi [3] who showed that the adding up of a small amount (less than 1% by volume) of nanoparticles to conventional heat transfer liquids enhance the thermal conductivity of the fluid up to approximately two times. The written work on nanofluid has been reconsidered by Trisakri and Wongwise [4]. These reviews examined the work done on convective transport in nanofluids. Nanofluids are described by enhanced thermal conductivity; a phenomenon observed by Masuda et al [5]. The unsteady nature of a broad range of fluid flows has been acknowledged over the past several years. In numerous applications, the ideal flow environment in the region of the device is nominally steady, but undesirable unsteady things crop up which are either self induced or due to fluctuations or non-uniformities in the neighboring fluid. The flow of Newtonian fluid over a

* Corresponding author
E-mail addresses: rajnish.bitpatna@gmail.com (Rajnish Kumar), rizvi.fauzia786@gmail.com (Fauzia Raza), msabel2001@yahoo.co.uk (M. Subhas Abel)

linearly stretching surface was analyzed by Crane [6]. The study of unsteady boundary layer owes its significance in the direction of the fact that all boundary layers, which take place in practice, are unsteady. Vajravelu et al [7] considered unsteady convective boundary layer flow of a viscous fluid at a vertical surface with variable fluid properties and they observed that an increment in the unsteady parameter causes thinning of the thermal boundary layer. Unsteady boundary layer flow over a stretching surface was considered by Misra et al [8]. Diverse aspects of the unsteady stretching sheet problem have been investigated by numerous authors [9-13]. The problem of unsteady two dimensional stagnation point flow and heat transfer of a viscous, compressible fluid at an accelerated flat plate was taken into consideration by Mozayyeni and Rahimi [14]. They analyzed that for a moving plate through an exponential velocity function towards the impinging flow the channel of time brings about a decrease in dimensionless heat transfer coefficient for any preferred value of wall temperature. Etwire et al [15] studied the consequences of MHD boundary layer stagnation point flow with radiation and chemical reaction towards a heated shrinking porous surface. The MHD radiating flow over an infinite vertical surface bounded by a porous medium in presence of chemical reaction was investigated by Ahmed and Kalita [16].

The objective of the present work is to study the outcome of various parameters namely, solid volume fraction, mixed convection parameter, unsteady parameter, Prandtl number, Lewis number, Brownian motion number, thermopheresis parameter and combined magnetic and porosity parameter on MHD mixed convection boundary layer flow over an unsteady surface in the presence of chemical reactions, non-uniform heat source and thermal radiation through a porous medium in CuO nanofluid.

Basic equations

Consider the unsteady two-dimensional mixed convectional boundary layer flow on a stretching sheet in an incompressible fluid. The fluid is a water based nanofluid having CuO nanoparticles. It is also supposed that the base fluid and nanoparticles are in thermal equilibrium and no slip arises among them. Let the x-axis is taken along the stretching surface in the path of motion and y-axis is normal to it. The plate is stretched along the x-direction with a velocity $U_w = \frac{ax}{1-\alpha t}$ defined at $y = 0$. A variable magnetic field $B(x) = \frac{B_0}{1-\alpha t}$ is applied normal to the sheet, B_0 being a constant. The thermo physical properties of regular fluid and CuO nanoparticles are given in Table 1.

Table 1: Thermophysical properties of water and Copper oxide

	P (kg/m³)	c_p (J/kg K)	k (W/mK)	β ×10⁻⁵ (1/K)
H_2O	997.1	4179	0.613	21.0
CuO	3620	531.8	76.500	1.80

The governing equations of the present problems are:

$$\frac{\partial u}{\partial x} + \frac{\partial v}{\partial y} = 0 \tag{1}$$

$$\frac{\partial u}{\partial t} + u\frac{\partial u}{\partial x} + v\frac{\partial u}{\partial y} = \frac{\mu_{nf}}{\rho_{nf}}\frac{\partial^2 u}{\partial y^2} + g\frac{\phi(\rho\beta)_s + (1-\phi)(\rho\beta)_f}{\rho_{nf}}(T - T_\infty) - \frac{\upsilon_{nf}}{K}u - \frac{\sigma B^2(x)}{\rho_{nf}}u \tag{2}$$

$$\frac{\partial T}{\partial t} + u\frac{\partial T}{\partial x} + v\frac{\partial T}{\partial y} = \alpha_{nf}\frac{\partial^2 T}{\partial y^2} + \tau\left\{D_B\frac{\partial c}{\partial y}\frac{\partial T}{\partial y} + \frac{D_T}{T_\infty}\left(\frac{\partial T}{\partial y}\right)^2\right\} - \frac{1}{(\rho c_p)_{nf}}\frac{\partial q_r}{\partial y} \tag{3}$$

$$\frac{\partial C}{\partial t} + u\frac{\partial C}{\partial x} + v\frac{\partial C}{\partial y} = D_B\frac{\partial^2 C}{\partial y^2} - \gamma(C - C_\infty) \tag{4}$$

q_r is the radiative heat flux, v_{nf} is the kinematic viscosity, $\mu_{nf} = \frac{\mu_f}{(1-\phi)^{2.5}}$ is the dynamic viscosity of the nanofluid, $\rho_{nf} = (1-\phi)\rho_f + \phi\rho_s$ is the density of the nanofluid,

$\alpha_{nf} = \frac{k_{nf}}{(\rho c_p)_{nf}}$ is the thermal diffusivity with k_{nf} is the thermal conductivity of the fluid, where $k_{nf} = k_f \frac{(k_s+2k_f)-2\phi(k_s-k_f)}{(k_s+2k_f)+\phi(k_s-k_f)}$, $c_p$is the heat capacity at constant pressure and $(\rho Cp)_{nf} = (\rho Cp)_f(1-\phi) + (\rho Cp)_s\phi$.

The radiative heat flux under rosseland approximation [17] has the form:

$$q_r = -\frac{4\sigma}{3k_1}\frac{\partial T^4}{\partial y}, \tag{5}$$

where k_1 and σ are the mean absorption coefficient and the Stefan-Boltzman constant.

We suppose that the temperature difference inside the flow is adequately small such that T^4 can be expressed as a linear function of temperature. Hence expanding T^4 in Taylor series about T_∞ and neglecting higher order terms, we get:

$$T^4 \cong 4T_\infty{}^3 - 3T_\infty{}^4 \tag{6}$$

Using (5) and (6), equation (3) reduces to:

$$u\frac{\partial T}{\partial x} + v\frac{\partial T}{\partial y} = \alpha_{nf}\frac{\partial^2 T}{\partial y^2} + \tau\left\{D_B\frac{\partial c}{\partial y}\frac{\partial T}{\partial y} + \frac{D_T}{T_\infty}\left(\frac{\partial T}{\partial y}\right)^2\right\} + \frac{16\sigma T_\infty{}^3\partial^2 T}{3k_1(\rho c_p)_{nf}\partial y^2} \tag{7}$$

The corresponding boundary conditions are:

$$u = U_w(x,t),\ \ v = 0, T = T_w(x,t)\ , C = C_w(x,t) \text{ at} y = 0$$
$$u \longrightarrow U(x),\ \ T \longrightarrow T_\infty\ \ , C \longrightarrow C_\infty \text{ at } y \to \infty. \tag{8}$$

Following Ishak et al. [18], the stretching velocity is considered as $U_w(x,t) = \frac{ax}{1-\alpha t}$, where a and α are constants (with a ≥ 0, $\alpha \geq 0$ such that αt< 1) and both have dimension t^{-1}. We have a as the initial stretching rate $\frac{a}{1-\alpha t}$ and it increases with time.

The temperature of the sheet is: $\quad T_w = T_\infty + \frac{bx}{(1-\alpha t)^2}$, (9)

where T_0 is the reference temperature, T_w is the surface temperature and T_∞ is the temperature of the fluid exterior the boundary layer. The wall surface concentration $C_w(x,t)$ is given by the expression:

$$C_w = C_\infty + \frac{bx}{(1-\alpha t)^2} \tag{10}$$

c_w is the wall surface concentration and C_∞ is the concentration of the fluid outside the boundary layer and $K = K_0(1-\alpha t)$.

Now introducing the following similarity transformations:

$$\eta = \left(\frac{a}{\nu}\right)^{1/2}(1-\alpha t)^{-1/2}y\,,\ \psi = (a\nu)^{\frac{1}{2}}(1-\alpha t)^{-1/2}xf(\eta) \tag{11}$$

$$\theta(\eta) = \frac{T-T_\infty}{T_W-T_\infty}, h(\eta) = \frac{C-C_\infty}{C_W-C_\infty}, \tag{12}$$

Where ψ is the stream function that satisfies Eq. (1) with:

$$u = \frac{\partial\psi}{\partial y} \text{ and } v = -\frac{\partial\psi}{\partial x} \tag{13}$$

In terms of these variables the velocity components can be expressed as:

$$u = \frac{ax}{1-\alpha t}f'(\eta),\qquad v = -\sqrt{\frac{a\nu}{1-\alpha t}}f(\eta) \tag{14}$$

Making use of similarity transformations, the governing equations take the form:

$$f''' - (1-\phi)^{2.5}\left\{1-\phi+\phi\frac{\rho_s}{\rho_f}\right\}\left[\begin{array}{c} f'^2 - ff'' - \\ A\left(f' + \frac{\eta}{2}f''\right) + Mf' + \left\{1-\phi+\phi\frac{(\rho\beta)_s}{\rho\beta_f}\right\}\zeta\theta \end{array}\right] \tag{15}$$

$$\theta'' + \frac{1}{(1+Nr)}Pr\frac{k_f}{k_{nf}}\left\{1-\phi+\phi\frac{(\rho Cp)_s}{(\rho Cp)_f}\right\}\left\{\begin{array}{c} f\theta' - f'\theta + Nbh'\theta' \\ +Nt\theta'^2 - A\left(2\theta + \frac{\eta}{2}\theta'\right) \end{array}\right\} = 0 \tag{16}$$

$$h'' + Le\left\{(f'h - fh') - A\left(2h + \frac{\eta}{2}h'\right) - \lambda h\right\} = 0 \tag{17}$$

And the transformed boundary conditions are:

$$f'(0) = \varepsilon, \theta(0) = 1,\ h(0) = 1\ at \eta = 0$$
$$f(0) = 0\ , \theta(0) = 0,\ h(0) = 0\ at \eta = \infty \qquad (18)$$

where ε is the stretching/shrinking parameter according as $\varepsilon > 0$ or $\varepsilon < 0$. $A = \frac{a}{\alpha}$ is the parameter that measures the unsteadiness.$Pr = \frac{\nu_f}{\alpha_f}$ is the Prandtl number, $Nr = \frac{16\sigma T_\infty{}^3}{3kk_1}$ is the parameter of radiation, $Le = \frac{\nu_f}{D_B}$ is the Lewis number, $Nb = \tau D_B \frac{(C_W - C_\infty)}{\nu_f}$ is the Brownian motion number, $Nt = \tau D_T \frac{(T_W - T_\infty)}{T_\infty \nu_f}$ is the thermopheresis number, $M = \frac{\sigma B_0{}^2}{a\rho_{nf}} + \frac{\nu_{nf}}{aK_0}$ is the combined magnetic and porosity parameter, $\lambda = \frac{\gamma}{b}(1 - \alpha t)$ is the instantaneous reaction rate parameter and $\zeta = \frac{gb\beta}{a^2}$ is a dimensionless constant with $\zeta > 0$ and $\zeta < 0$ correspond to assisting and opposing flows respectively and $\zeta = 0$ is for forced convection flow situation.

The physical quantities of interest are the skin friction coefficient, the local Nusselt number and Sherwood number which are defined as:

$$C_f = \frac{\mu}{\rho_f U_W^2}\left(\frac{\partial u}{\partial y}\right)_{y=0} \qquad (19)$$

$$Nu = \frac{x}{k(T_W - T_\infty)}\left[k\left(\frac{\partial T}{\partial y}\right)_{y=0} - \frac{4\sigma}{3k_1}\left(\frac{\partial T^4}{\partial y}\right)_{y=0}\right] \qquad (20)$$

$$Sh = -\frac{x}{(C_W - C_\infty)}\left(\frac{\partial C}{\partial y}\right)_{y=0} \qquad (21)$$

with μ and k are the dynamic viscosity and thermal conductivity, respectively. Using non-dimensional variables, we have:

$$C_f Re_x^{1/2} = f''(0) \qquad (22)$$
$$NuRe_x^{1/2} = -(1 + \mathrm{Nr})\theta'(0) \qquad (23)$$
$$Re_x^{1/2} Sh = -\phi'(0) \qquad (24)$$

Methods of Solution

The set of non-linear differential equations (15)-(17) with boundary conditions (18) constitute a two–point boundary value problem. These highly non-linear differential equations cannot be solved analytically. As a result, these equations are solved by the software MATLAB function “bvp4c”. The function has three key variables: the name of the M-file enumerating an ordinary differential equation system of the design, the term of the M-file enumerating the boundary values, and an initial approximation of the result prepared with the MATLAB function “bvpinit”.

Results and Discussion

The numerical solutions of governing equations are solved by using the function ‘bvp4c’ of MATLAB. To certify our result, the numerical computations of skin friction, Nusselt number and Sherwood number are presented in tabular form and the comparison is done with Nazar et al [19] and Lok et al [20] for skin friction and Nusselt number. There is an excellent agreement of the results obtained with them.

Table 2: Comparison between present study and previous reported results when =0, ζ=1.

Pr	Nazar et al [19]		Lok et al [20]		Present result	
	$f''(0)$	$-\theta'(0)$	$f''(0)$	$-\theta'(0)$	$f''(0)$	$-\theta'(0)$
0.7	1.7063	0.7641	1.706376	0.764087	1.076203	0.764054
7	1.5179	1.7224	1.517952	1.722775	1.517913	1.722371
10	-	-	-	-	1.492842	1.944609
60	1.3903	3.5514	1.390311	3.355404	1.390278	3.551417
90	-	-	-	-	1.372393	4.066227
100	1.3680	4.2116	1.368070	4.218462	1.368043	4.211689

To analyse the consequence, Numerical computations have been conceded for the velocity, temperature and concentration profile for diverse governing parameters namely, unsteadiness parameter A, combined magnetic and porosity parameter M, mixed convection parameter ζ, Solid volume fraction ϕ, Prandtl number Pr,radiadion parameter Nr, thermopheresis parameter Nt, Brownian motion number Nb, Lewis number Le and varying reaction rate parameter λ on the coefficient of skin friction coefficient, Nusselt number and Sherwood number correspondingly. The skin friction coefficient $f''(0)$ rises with the rise in solid volume fractionϕ. It is also observed that the local Nusselt number decreases while Sherwood number enhances with enhancement in solid volume fractionϕ.

Fig. 1-Fig. 4 shows the variation in velocity profile intended for combined magnetic and porosity parameter$M$, unsteadiness parameter A, mixed convection parameter ζ and solid volume fraction ϕ respectively. It is obvious from Fig. 1 that the velocity profile decrease by increase in value of η tends asymptotically to zero. Fig. 2 illustrates that the velocity profile is increased with increase in mixed convection parameter ζ. Fig. 3 shows that the velocity profile is decreased with increase in A once more it decreases to zero. Fig. 4 exhibits that the velocity profile is decreased and it is extreme at $\phi = 0.1$. This happens due to the presence of solid nano-particles which leads to further thinning of the velocity boundary layer thickness.

Fig. 5-Fig. 10 is for variation in temperature profile for diverse parameters. Fig. 5 is for variation in solid volume fractionϕ on temperature profile. The temperature profile decline with increase in η and the thickness of boundary layer also increases. Fig. 6 is for variation in Prandtl number Pr on temperature profile. The temperature profile decreases with raise in Pr and the thickness of boundary layer is also declined. Fig. 7 is for variation in unsteadiness parameter A and it is obvious from the figure that the temperature profile increases with increase in A and thermal boundary layer thickness also rises. Fig. 8 is aimed at variation in thermal radiation Nr on temperature profile. The fluid temperature decreases with increase in Nr. This reality disclosed the result that the decrease in value of $Nr\left(=\frac{16T_\infty^3\sigma}{kk_1}\right)$ for given $k$and T_∞ means an enhancement in Rosseland absorptivity k_1. According to equations (3) and (5), the divergence of the radiative heat flux $\frac{\partial q_r}{\partial y}$ decreases as $k_1$increases which in turn decrease the rate of heat transferred to the fluid and hence the fluid temperature decreases and thermal layer also decreases with increase in Nr.

Fig. 9 is for deviation in thermopheresis parameter Nt taking placeon temperature profile. It is visible from the figure that the fluid temperature rises with rise inNt in the boundary layer region and, as a result, thickness of boundary layer also increased as thermopheresis assists nanoparticle diffusion in the boundary layer. Fig. 10 is for variation in Brownian motion number Nb on temperature profile. Figure itself shows that the temperature profile increases with an increment in Nb as well as it decreases with increase in η.Their is an increment in thermal boundary layer thickness as well. Therefore, the distribution of nanoparticles in the flow regime can be arranged by the Brownian motion mechanism and the thermal boundary layer thickness increased.

Fig. 11-Fig. 13 is for variation in variant parameters on concentration profile. Fig. 11 shows that the temperature profile decreases with increase in unsteadiness parameter A and the boundary layer is also declined. Fig. 12 is for deviation in Lewis number Le on concentration profile and it depicted that the concentration profile decreased as Le increases as well as boundary layer is also decreased. Fig. 13 is for varying reaction rate parameter λ and figure itself shows that the concentration profile is decreased as rise in value of λ as well as boundary layer is also decreased. Fig. 14 and Fig. 15 are for variation in Nusselt number and Sherwood number respectively.

Table 3. Skin friction coefficient, local Nusselt number, Sherwood number for ζ=0.1, Pr=3, =0.1,A=0.2, M=0.2, Nt=Nb=0.5, Nr=0.4, Le=2

ϕ	$f''(0)$	$-\theta'(0)$	$-h'(0)$
0.0	-0.0917	0.5139	0.7686
0.1	-0.0614	0.4595	0.7971
0.2	-0.0405	0.4091	0.8273
0.3	-0.0259	0.3610	0.8583
0.4	-0.0159	0.3154	0.8887
0.5	-0.0092	0.2724	0.9175

Conclusion

In this paper, the consequences of MHD mixed convection boundary layer flow over an unsteady stretching surface with chemical reaction, non-uniform heat source and thermal radiation through a porous medium in CuO nanofluid has been analyzed. The investigation is performed for variant mentioned parameters and some conclusions are summarized as follow:

- The thermal boundary layer thickness decreased as Prandtl number increased.
- The Sherwood number is greatest at $\phi = 0.5$.
- The local Nusselt number is highest at $\phi = 0.0$.
- The temperature profile increases with increase in Brownian motion number Nb.
- The divergence of the radiative heat flux decreases as Rosseland absorptivity increases which in turn decrease the rate of heat transferred to the fluid.

References

1. Das, S.K., Choi, S.U.S., Yu, W., Pradeep. T. (2007). Nanofluids: Science and Technology, Wiley, NJ: Hoboken.
2. Wang, X.Q., Majumdar, A.S. (2008). A Review on Nanofluids-Part 1: Theoretical and Numerical investigations, Braz. J. Chem. Eng. 25(4): 613-630.
3. Choi, S.U.S. (1995). Enhancing thermal conductivity of fluids with nanoparticles. In: Siginer DA, Wang HP (eds). Development and applications of non-newtonian flows. ASME MD, vol. 231 and FED, vol. 66. USDOE, Washington, DC: 99-105.
4. Trisaksri, V., Wongwises, S. (2007). Critical review of heat transfer characteristics of nanofluids. Renew Sustain Energ Rev, 11:512-523.
5. Masuda, H., Ebata, A., Teramae, K., Hishinuma, N. (1993). Alteration of thermalconductivity and viscosity of liquid by dispersing ultra-fine particles, NetsuBussei. Retrieved from http://www.jstage.jst.go.jp.
6. Crane, L.J. (1977). Flow past a stretching plate. Z. Angew. Maths. Phys. 55: 744-746.
7. Vajravelu, K., Prasad, K.V., Ng, Chiu-On. (2013). Unsteady convective boundary layer flow of a viscous fluid at a vertical surface with variable fluid properties. Real world Applications, 14: 455-464.
8. Misra, M., Ahmad, N., Siddiqui, Z.U. (2012). Unsteady Boundary Layer Flow past a Stretching Plate and Heat Transfer with Variable Thermal Conductivity. World Journal of Mechanics, 2: 35-41.
9. Chiriac, V.A., Ortega, A. (2002). A Numerical Study of the Unsteady Flow and Heat Transfer in a Transitional Confined Slot Jet Impinging on an Isothermal Surface. Int. J. Heat and Mass Transfer, 45: 1237-1248.
10. Sau, A., Nath, G. (1995). Unsteady Compressible Boundary Layer Flow On the Stagnation Line of an Infinite Swept Cylinder, Acta Mech. 108:143-15.
11. Kumari, M., Nath, G. (1980). Unsteady Compressible 3- Dimensional Boundary Layer Flow Near a Asymmetric Stagnation-Point with Mass Transfer. Int J. Eng. Sci. 18: 1285-1300.
12. Kumari, M., Nath, G. (1981). Self Similar Solution of Unsteady Compressible 3-Dimensional Stagnation Point Boundary Layers. J. Appl. Math. Phys. 32: 267-276.
13. Abbasi, A.S., Rahimi, A.B., Niazaman, H. (2011). Exact Solution of Three Dimensional Unsteady Stagnation –Point Flow on a Heated Plate. J. Thermodyn. Heat Transfer, 25:55-58.

14. Mozayyeni, H.R., Rahimi, A.B. (2014). Unsteady two dimensional stagnation point flow and heat transfer of a viscous, compressible fluid on an accelerated plate. Journal of Heat Transfer. 136.

15. Etwire, C.J., Seini, Y.I., Arthur, E.M. (2014). MHD Boundary Layer Stagnation Point Flow with Radiation and Chemical Reaction towards a Heated Shrinking Porous Surface‖, International Journal of Physical Science 9(14):320 – 328.

16. Ahmed,S., Kalita, K. (2013). Analytical and Numerical Study for MHD Radiating Flow over an Infinite Vertical Surface Bounded by a Porous Medium in Presence of Chemical Reaction‖ Journal of Applied Fluid Mechanics, Vol. 6, No. 4: 597-607.

17. Brewster, M.Q. (1992). Thermal Radiative Transfer Properties, Wiley, Canada.

18. Ishaq, R., Nazar, R., Pop, I. (2005). Boundary layer flow and heat transfer over an unsteady stretching vertical surface, Meccanica 44: 369-375.

19. Lok, Y.Y., Amin, N., Campean, D., Pop, I. (2005). Steady mixed convection flow of a micropolar fluid near the stagnation point on a vertical surface, Int J. Numerical Methods Heat Fluid Flow, 15: 654-670.

20. Ishak, A., Nazar, R., Pop, I. (2008). Post- stagnation- point boundary layer flow and mixed convection heat transfer over a vertical, linearly stretching sheet, Arch. Mech. 60(4): 303-322.

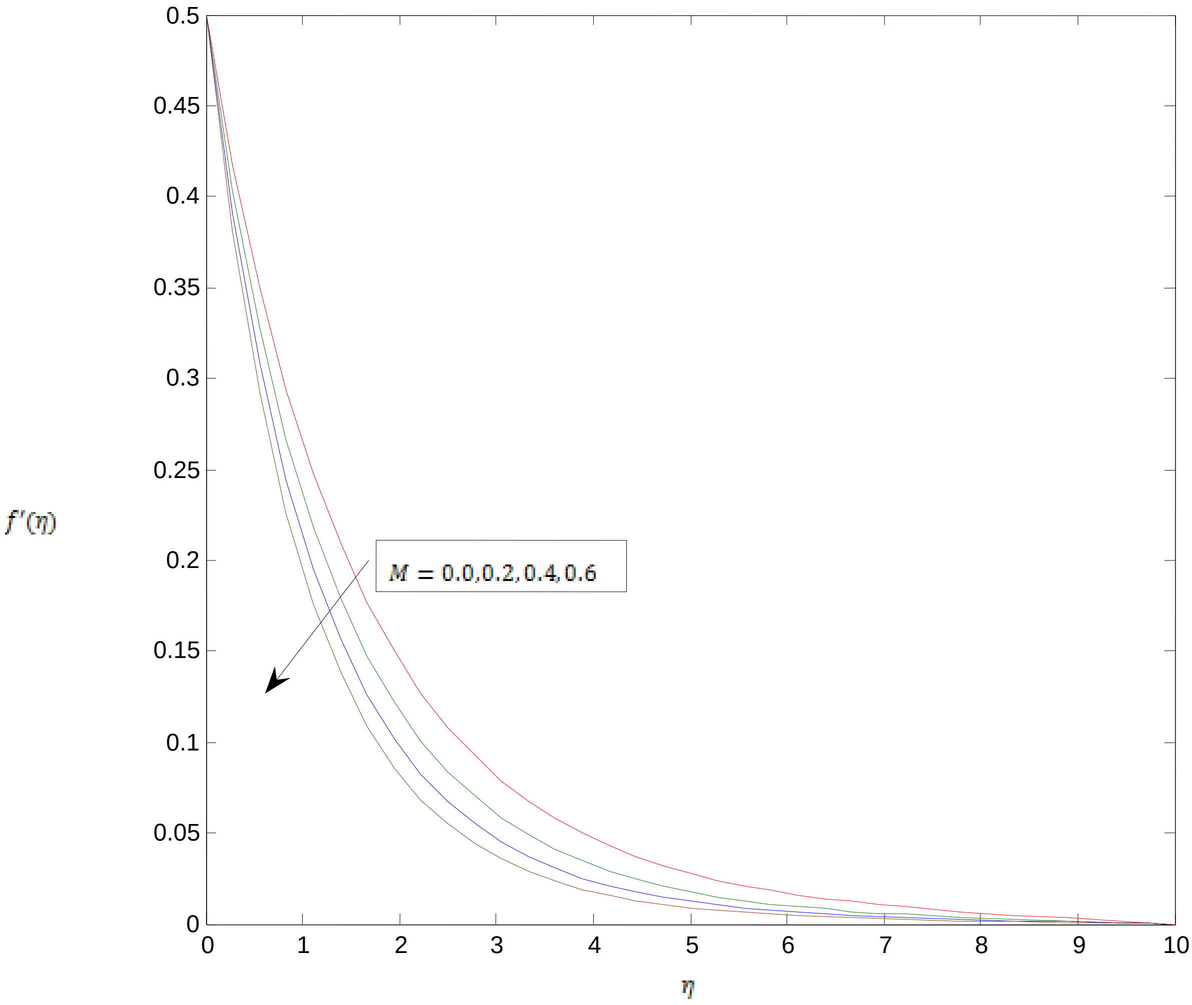

Figure 1: M=0.0, 0.2, 0.4, 0.6, ϕ=0.1, A=0.2, ζ=0.2,=0.5. Velocity profile for different values of porosity parameter M.

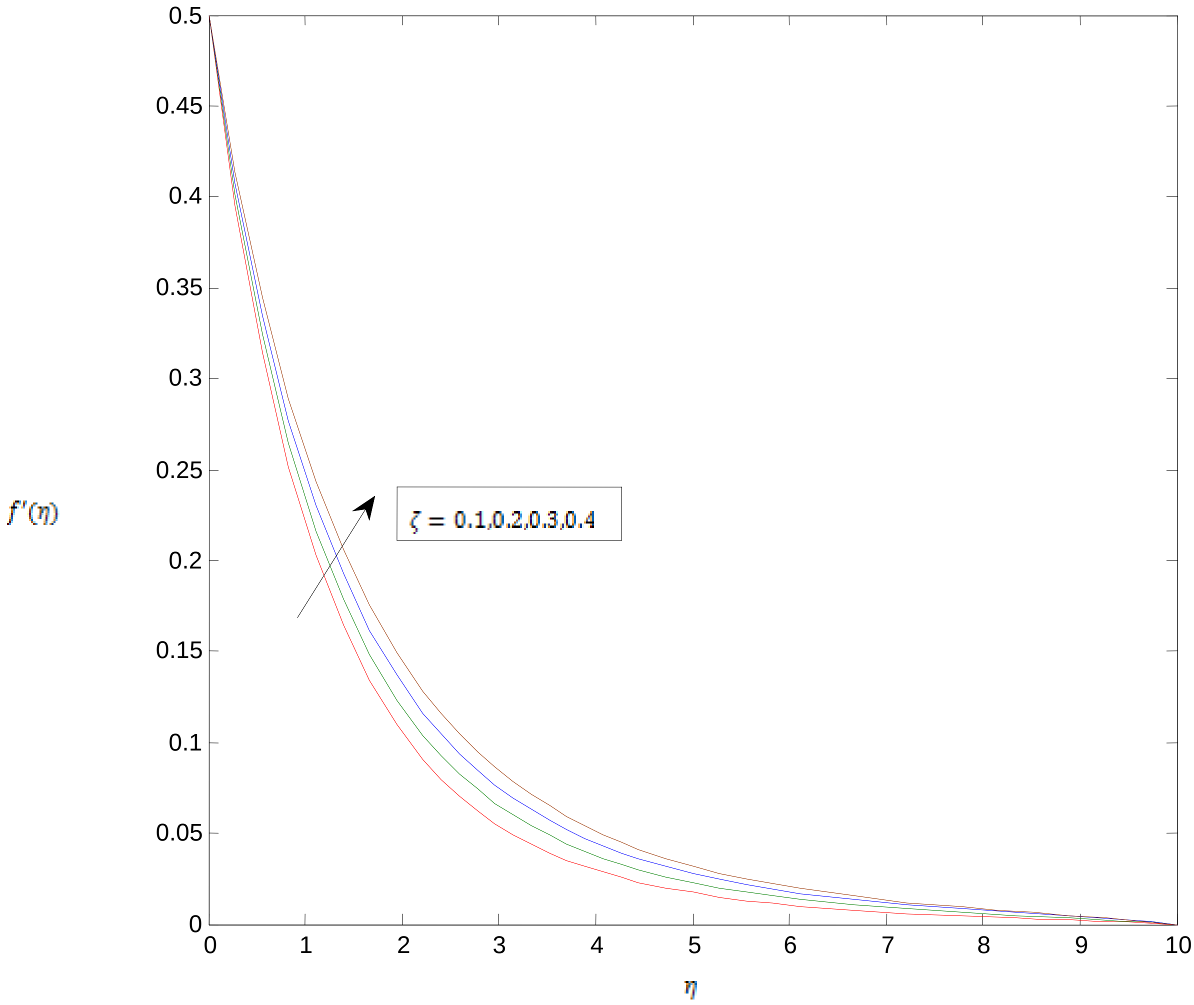

Figure 2: ζ =0.1, 0.2, 0.3, 0.4, M=0.2, ϕ=0.1, A=0.2, ε=0.5.Velocity profile for different values of mixed convection parameter ζ.

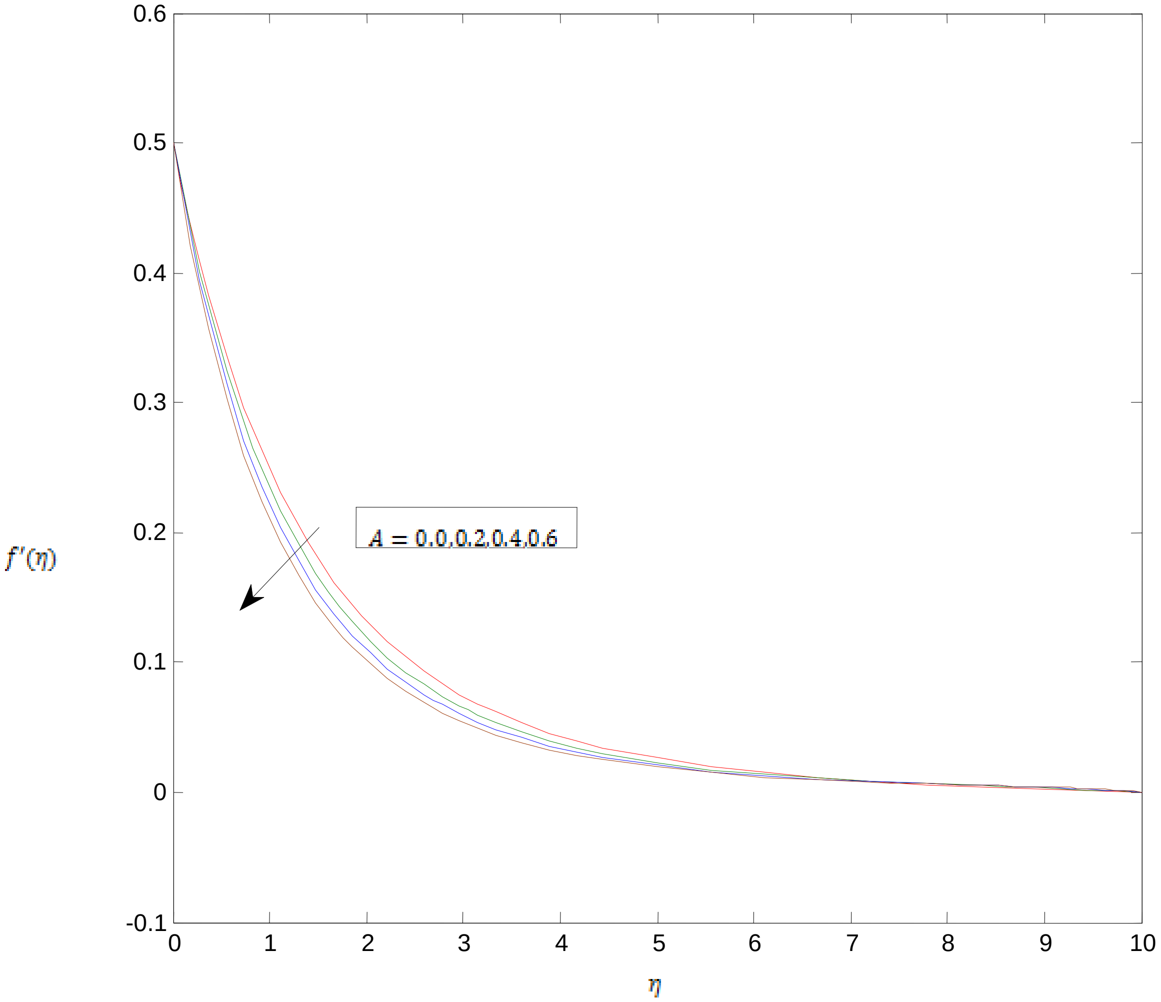

Figure 1: A=0.0, 0.2, 0.4, 0.6, M=0.2, ζ=0.2, A=0.2, ϕ=0.1, ε=0.5.Velocity profile for different values of unsteadiness parameter A.

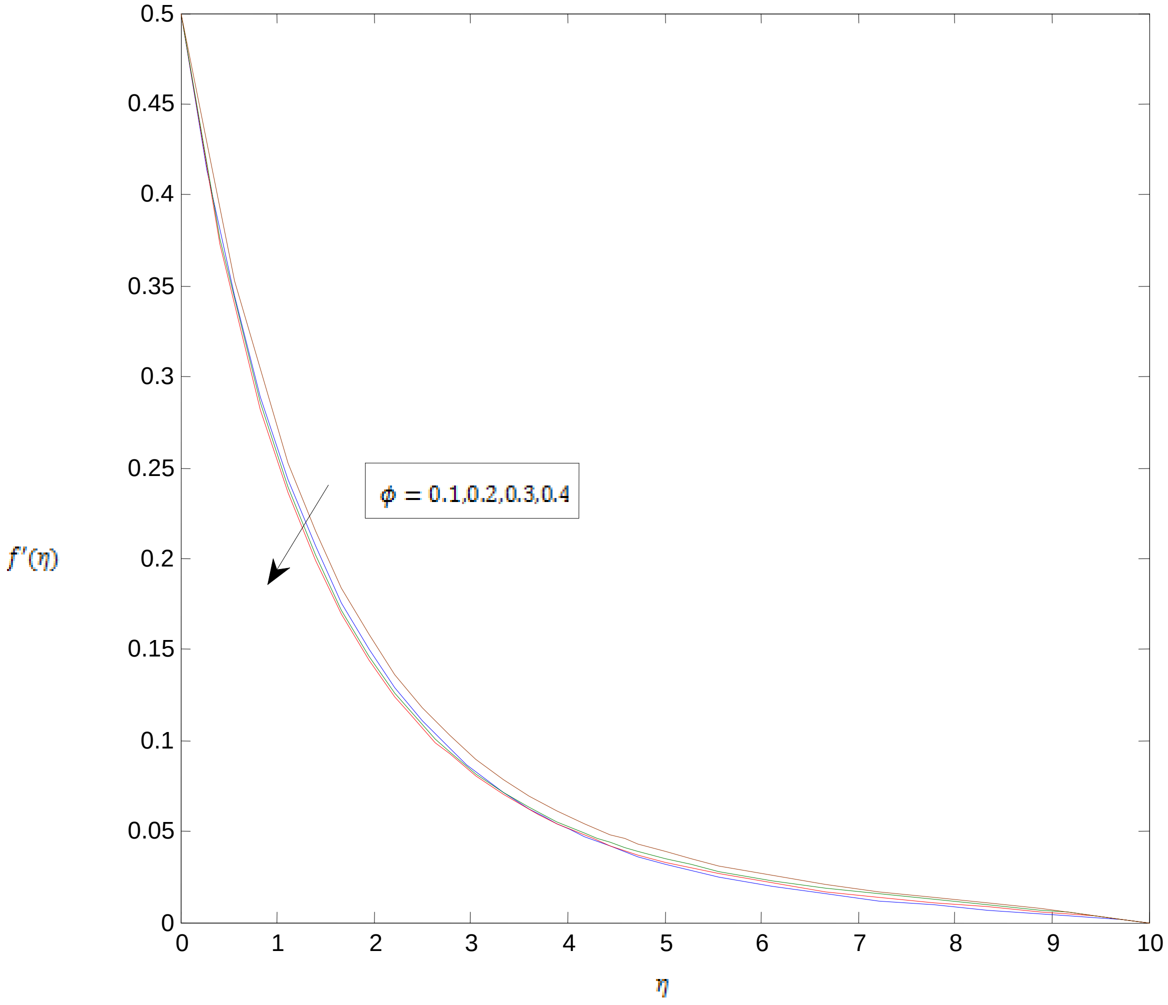

Figure 4: ϕ=0.1, 0.2, 0.3, 0.4, A=0.2, M=0.2, ζ=0.4, **ε**=0.5. Velocity profile for different values of solid volume fraction ϕ

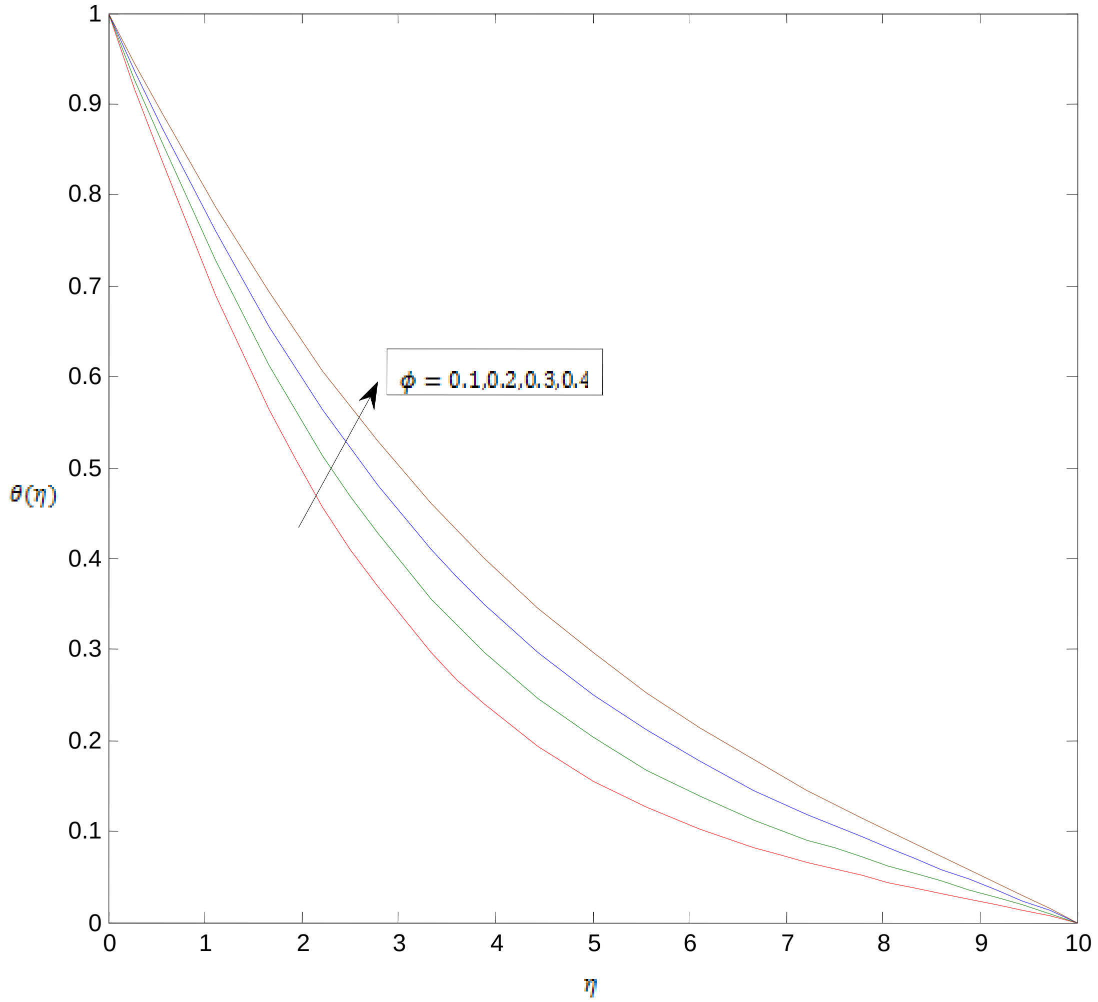

Figure 5: ϕ=0.1, 0.2, 0.3, 0.4, A=0.2, Pr=1, Nr=Nt=Nb=0.5, Le=1.Temperature profile for different values of solid volume fraction ϕ.

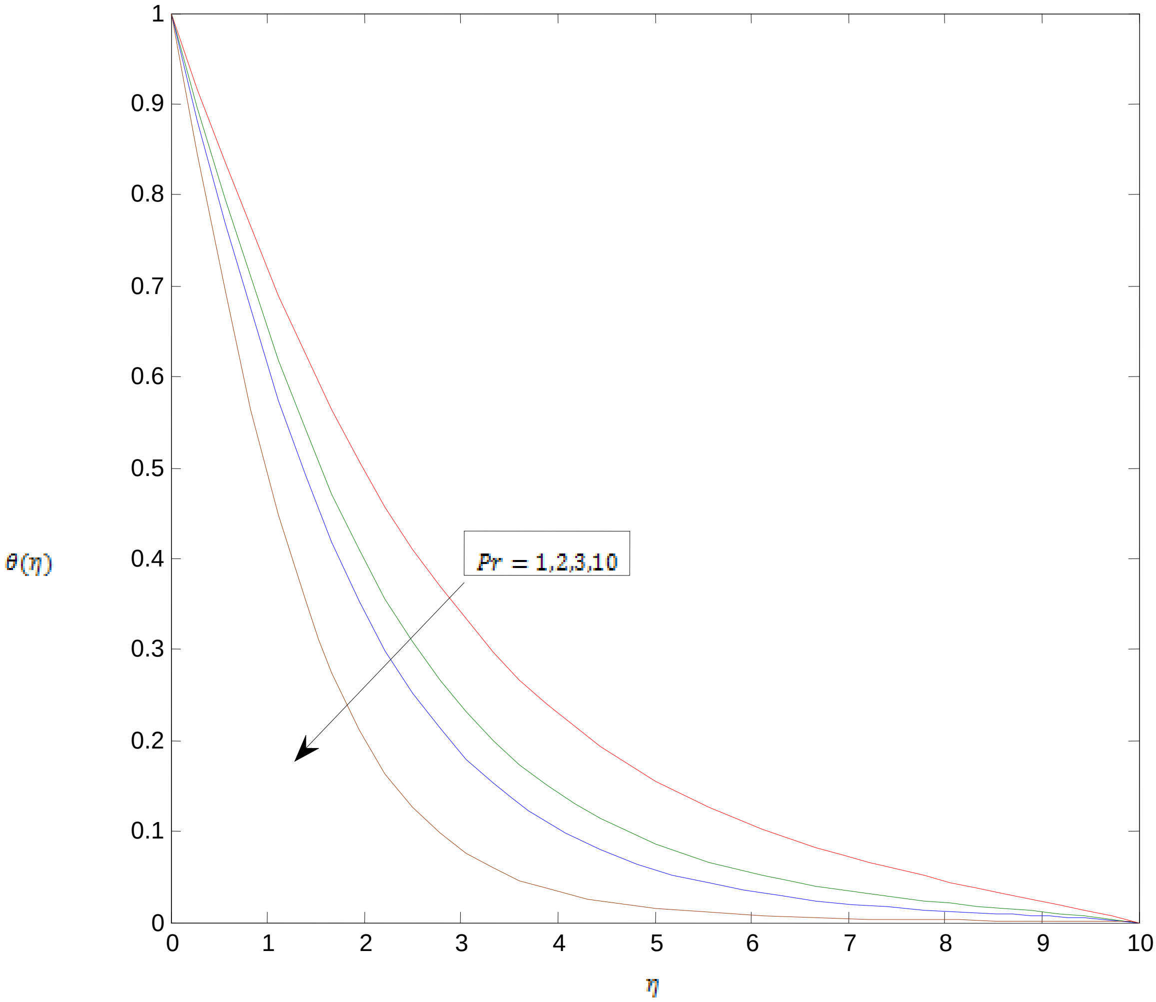

Figure 6: Pr=0.72, 1, 3, Nr=0.5, A=1.5, Nr=Nt=Nb=0.5, Le=1,ϕ=0.1. Temperature profile for different values of Prandtl number Pr.

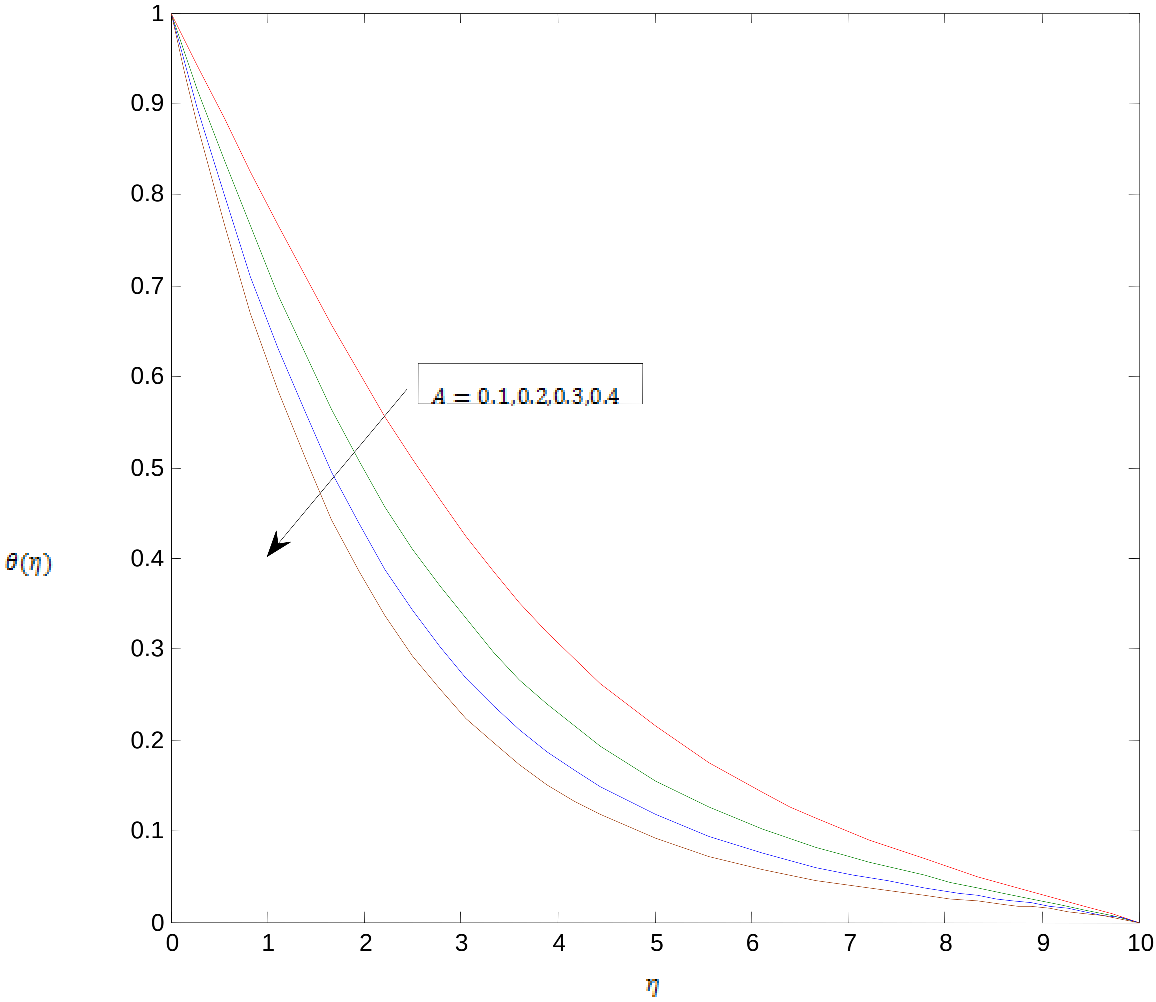

Figure 7: A=0.1, 0.2, 0.3, 0.4, Pr=1, Nr=Nt=Nb=0.5, Le=1, ϕ=0.1. Temperature profile for different values of unsteadiness parameter A.

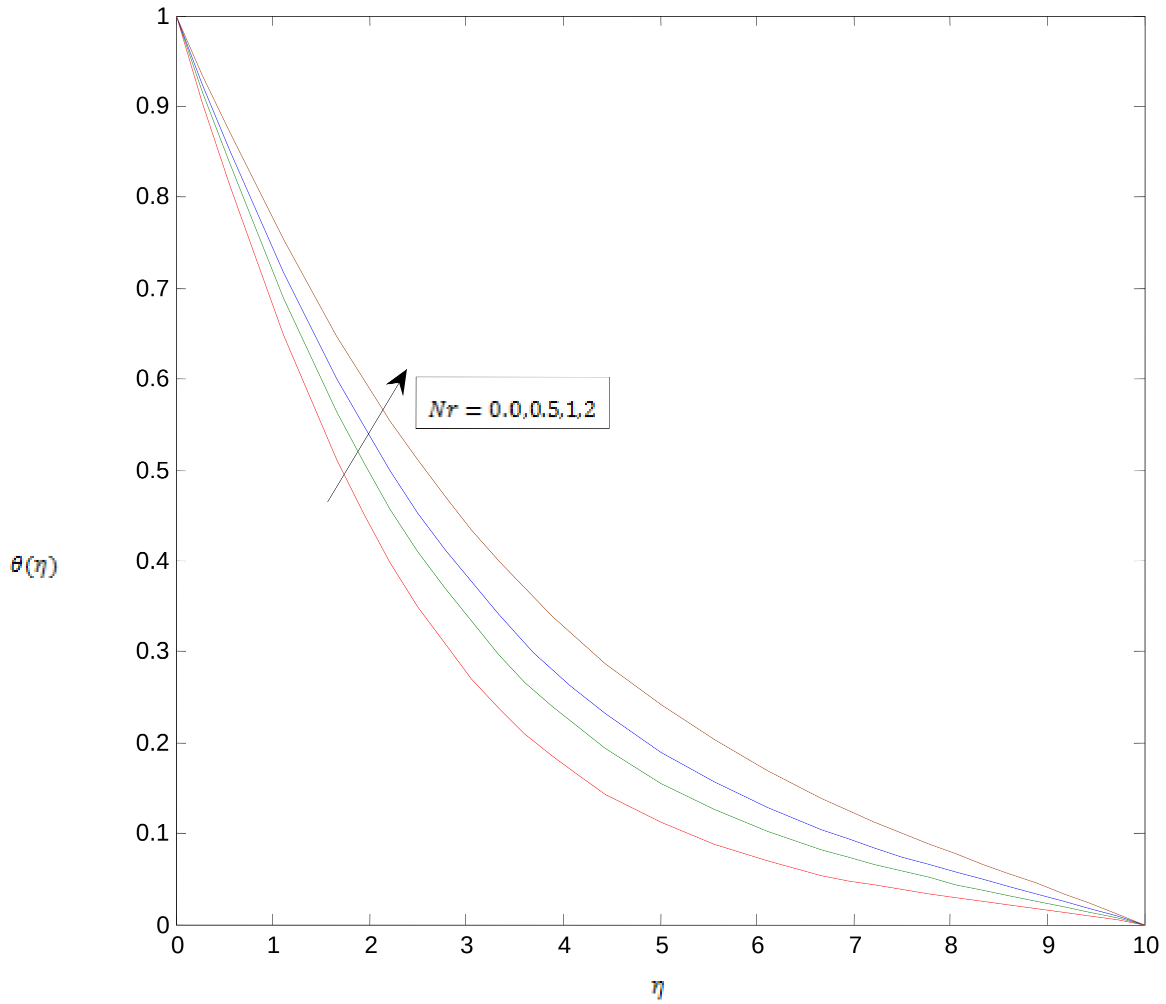

Figure 8: Nr=0.0, 0.5, 1, 2, ϕ=0.1, A=0.2, Pr=1,Nt=Nb=0.5, Le=1.Temperature profile for different values of radiation parameter Nr.

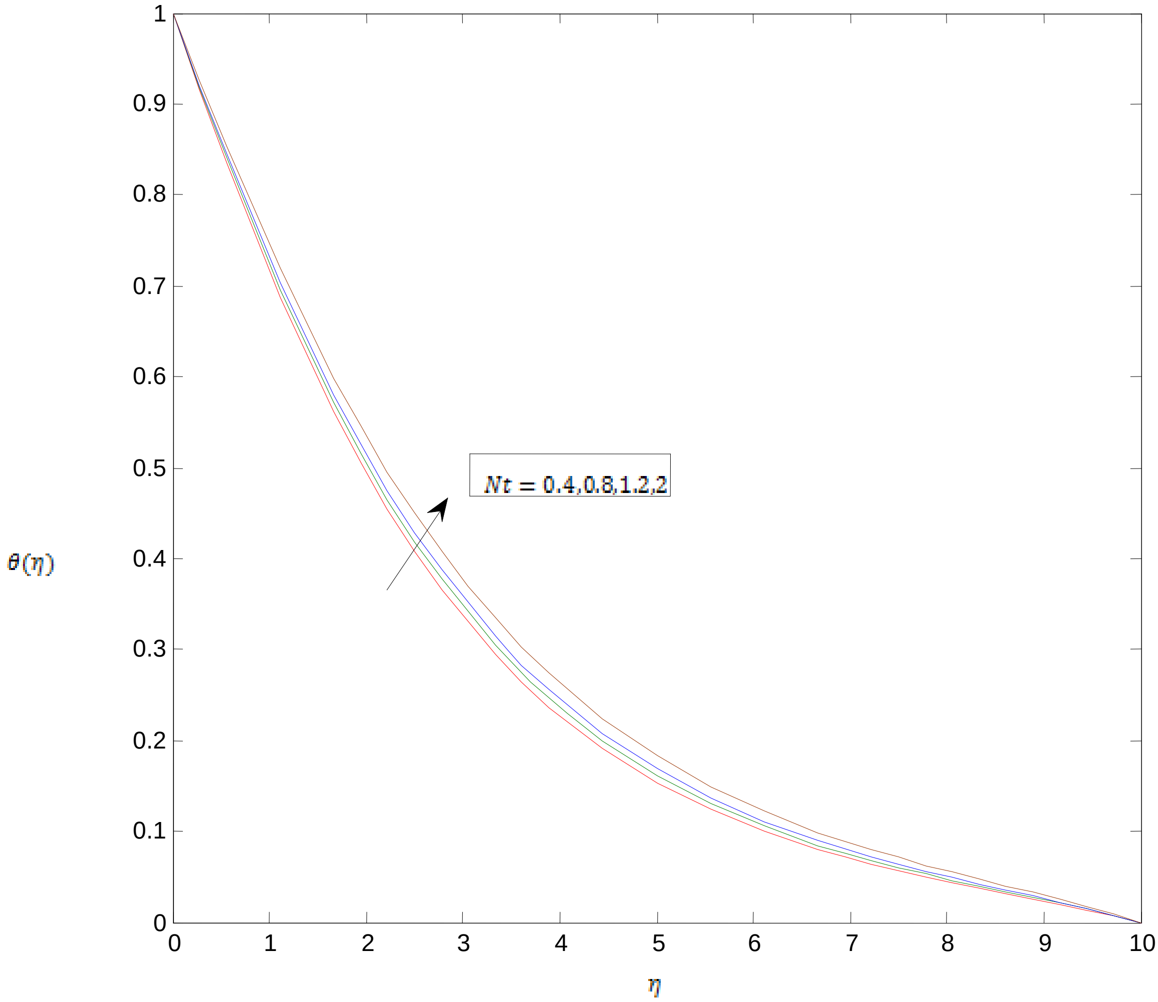

Figure 9: Nt= 0.4, 0.8, 1, 2, A=0.2, Pr=1,ϕ=0.1, Nr=Nb=0.5, Le=1.Temperature profile for different values of thermopheresis number Nt.

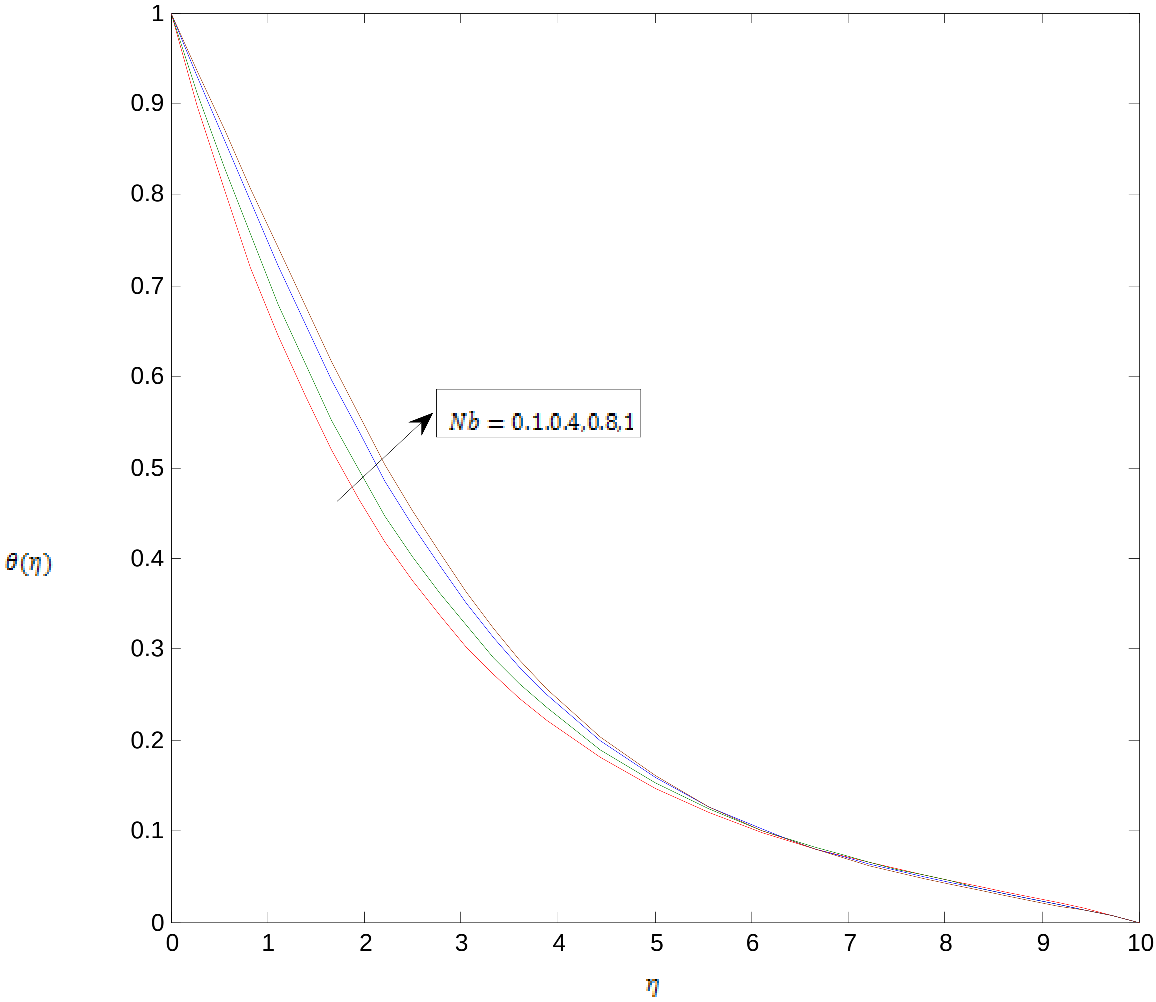

Figure 10: Nb= 0.1, 0.4, 0.8, 1, A=0.2, Pr=1,ϕ=0.1, Nr=Nt=0.5, Le=1.Temperature profile for different values of Brownian motion number Nb.

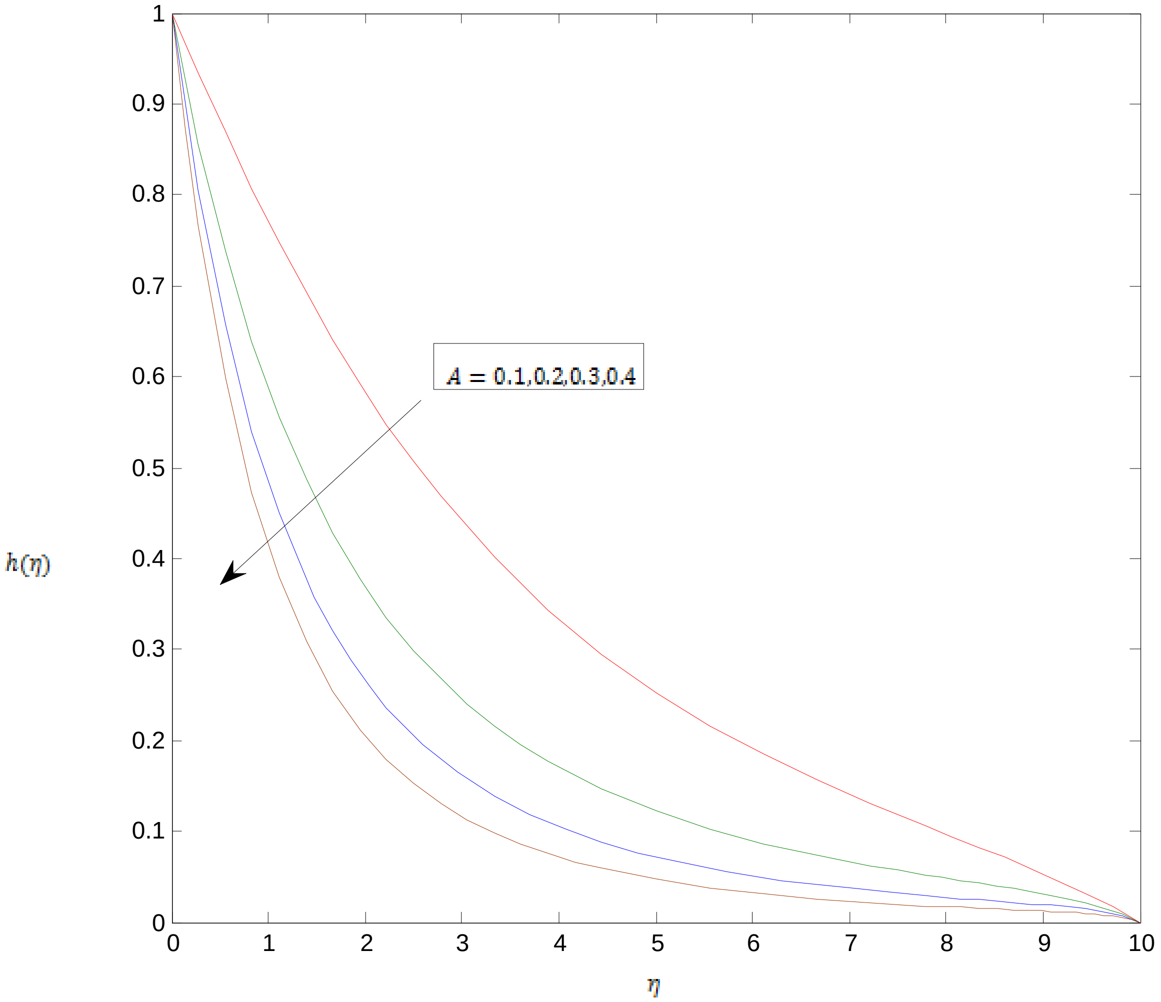

Figure 11: A=0.1, 0.2, 0.3, 0.4, $\boldsymbol{\lambda}$=-0.2, Le=2. Concentration profile for variation in unsteady parameter A.

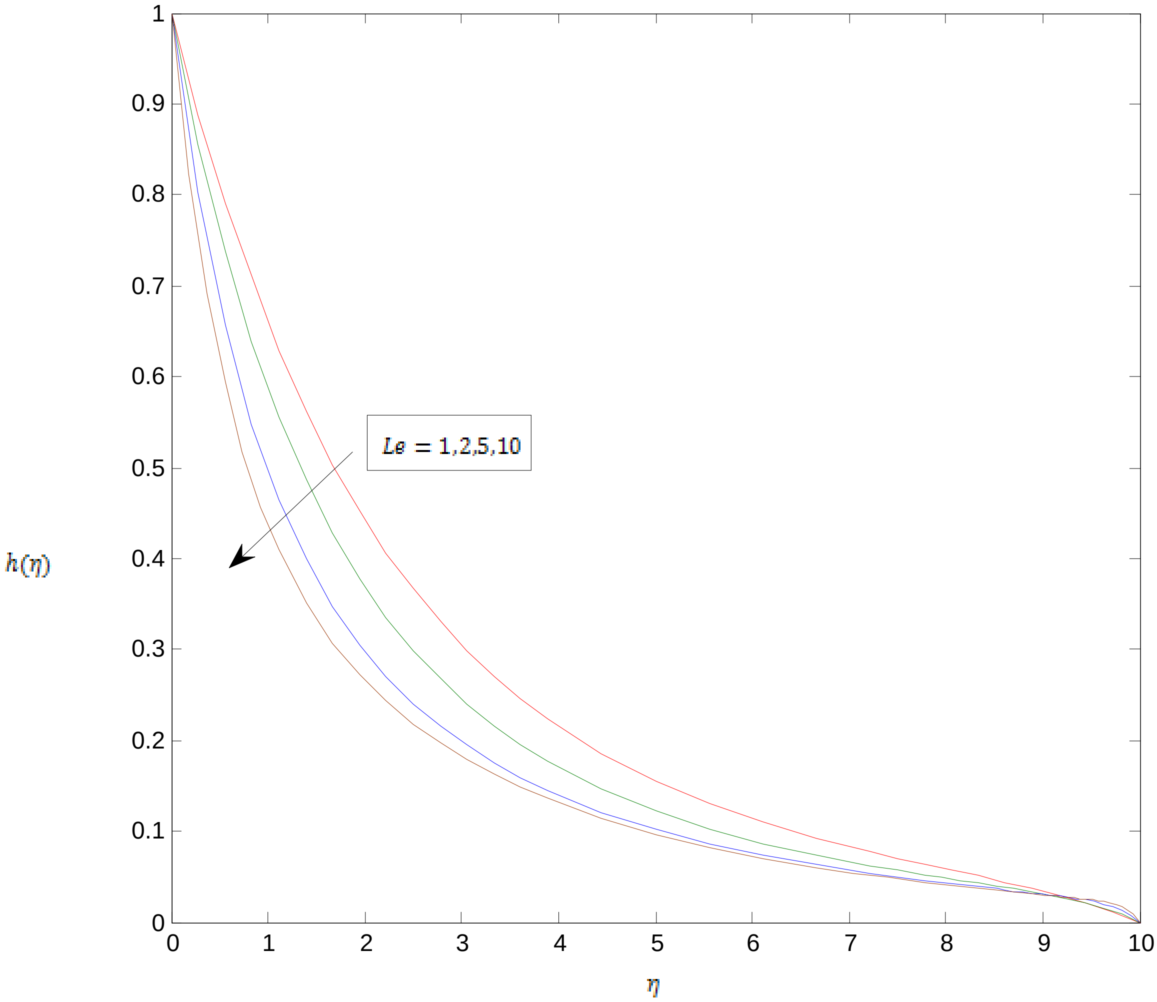

Figure 22: Le=1, 2, 5,10 ,A=0.2, $\boldsymbol{\lambda}$=-0.2. Concentration profile for variation in Lewis number Le

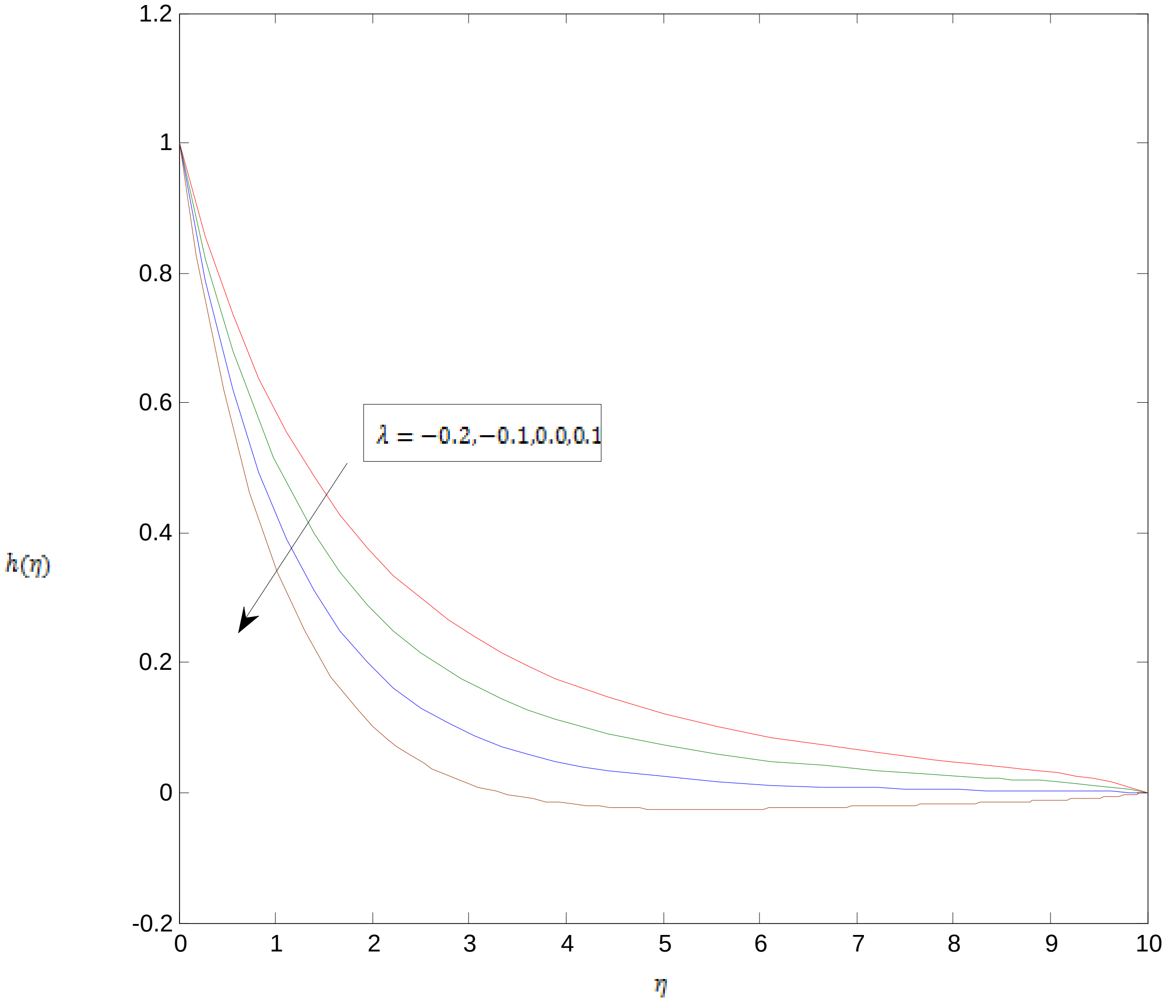

Figure 13: $\boldsymbol{\lambda}$=-0.2, -0.1, 0.0, 0.1, A=0.2, Le=2. Concentration profile for variation in varying reaction rate parameter$\boldsymbol{\lambda}$.

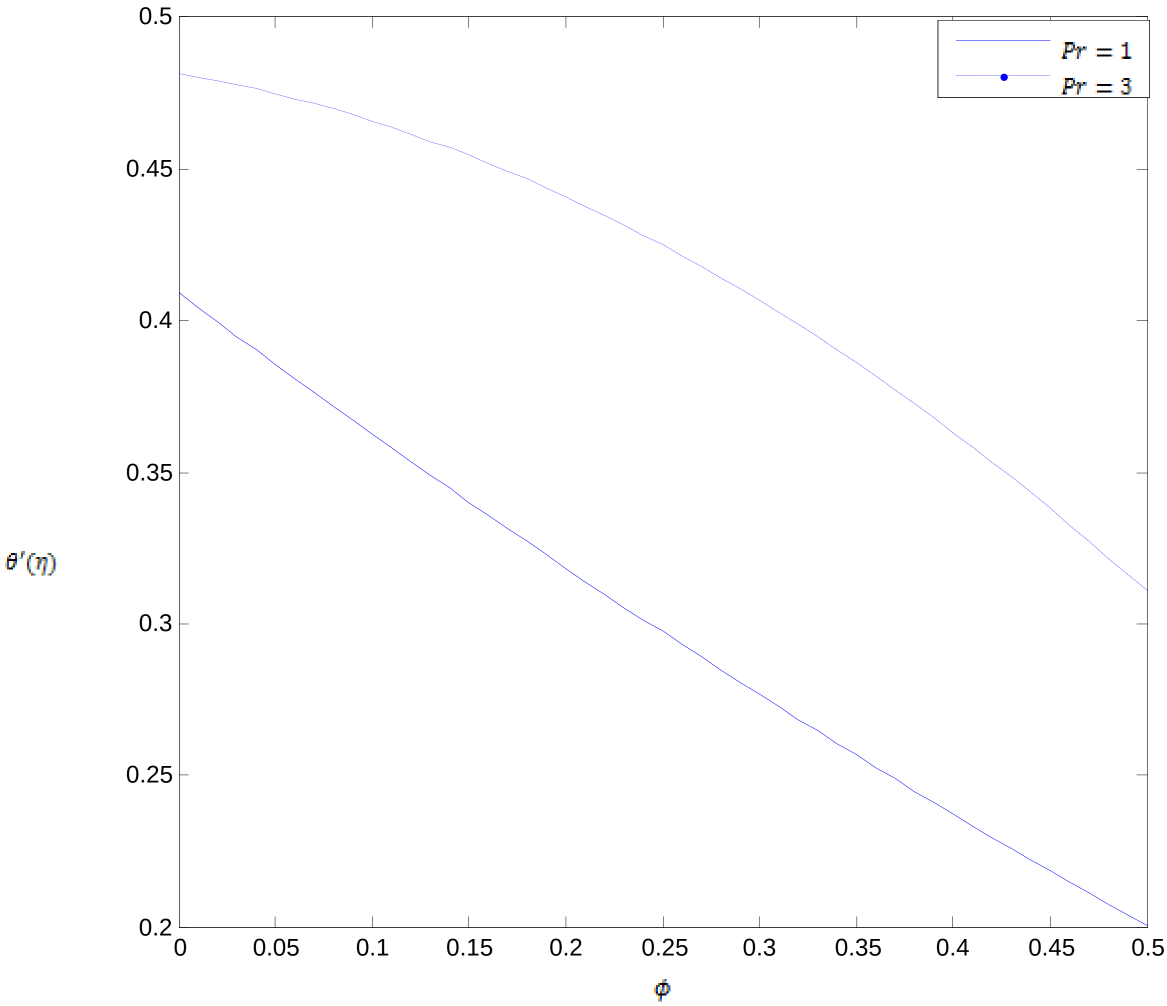

Figure 14: Nusselt number against different values of φ.

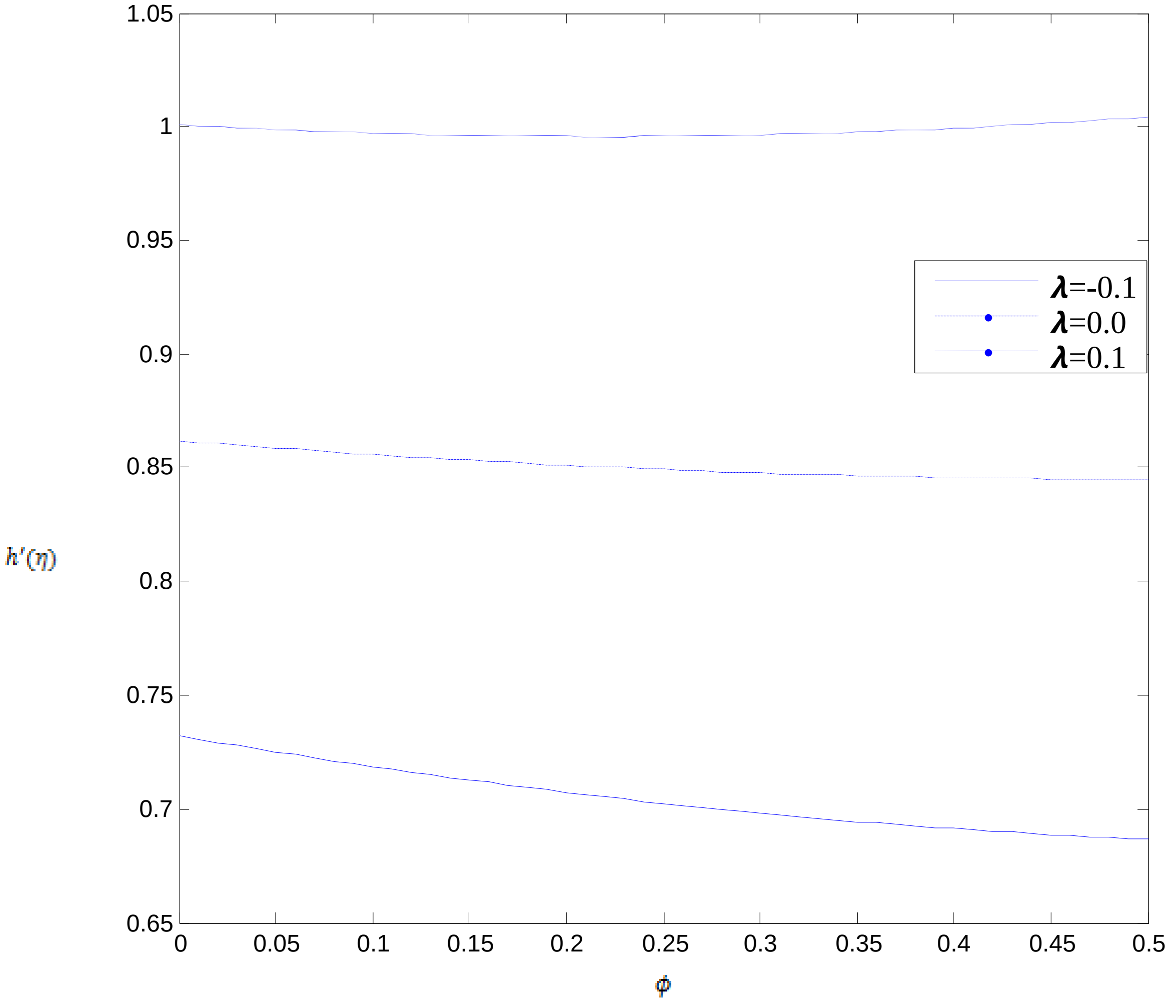

Figure 15: Sherwood number against different values of φ.